Mechatronics and Intelligent Transportation Systems
https://www.acadlore.com/journals/MITS

Simulation Analysis of Track Irregularity in High-Speed Maglev Systems Based on Universal Mechanism Software

Xiangyang Jia[1], Haiyan Qiang[1, 2*], Cheng Xiao[1], Chenglin Zhuang[1], Pengyu Yang[3], Xueyan Gao[4], Sumei Wang[5]

[1] Logistics Engineering College, Shanghai Maritime University, 201306 Shanghai, China
[2] Key Laboratory of Railway Industry of Maglev Technology, 201804 Shanghai, China
[3] Institute of Rail Transit, Tongji University, 201804 Shanghai, China
[4] University of Florida, 32611 Gainesville, USA
[5] National Rail Transit Electrification and Automation Engineering Technology Research Center (Hong Kong Branch), 999077 Hong Kong SAR, China

[*] Correspondence: Haiyan Qiang (hyqiang@shmtu.edu.cn)

Received: 10-26-2023 **Revised:** 12-02-2023 **Accepted:** 12-11-2023

Citation: X. Y. Jia, H. Y. Qiang, C. Xiao, C. L. Zhuang, P. Y. Yang, X. Y. Gao, and S. M. Wang, "Simulation analysis of track irregularity in high-speed Maglev systems based on universal mechanism software," *Mechatron. Intell Transp. Syst.*, vol. 2, no. 4, pp. 236–249, 2023. https://doi.org/10.56578/mits020405.

Abstract: As high-speed magnetic levitation (Maglev) technology continues to advance, the safety, stability, and passenger comfort of high-speed Maglev trains during operation are subject to increasingly stringent requirements. In this background, this study attempts to develop a stability simulation model for high-speed Maglev vehicles travelling at different speeds using the software Universal Mechanism (UM) and give a comprehensive analysis. High-speed Maglev trains are now an advanced mode of transportation, they possess many advantages including high safety, low emissions, low energy consumption, less noise, and stronger climbing capabilities. The safety, stability, and comfort level of high-speed Maglev trains are closely related to their operational speed and the irregularities of the tracks. This study takes the Shanghai TR08 Maglev train as the subject and models it in the UM to simulate and analyze the subject. With the help of this model, the responses given by the subject to track irregularities when it runs at different speeds are simulated, and the changes in stability metrics such as the Sperling Index are analyzed. After that, this study also investigates the relationship between operational speed, track irregularity, and stability, and the findings of this study could provide valuable insights for optimizing the design of high-speed Maglev trains and controlling of track irregularities.

Keywords: High-speed Maglev train; Dynamic modeling; Track irregularity; Stability index

1 Introduction

Maglev trains are now considered as a brand new form of rail transport with very good developmental prospects. Their operation principles and structural designs are very different from the old fashioned wheel-rail trains. Although the latter has seen rapid advancements in recent years, with top speed reaching 350 km/h, its speed limit is constrained by the adhesion of wheel-rail interactions [1]. As the speed increases, the mechanical noise and vibrations caused by the contact between wheels and rails can seriously decrease the passengers' comfort feeling and thus exert a impact on the environment along the railway lines. Besides, the mechanical wear of wheels and rails increases obviously as well, increasing the workload required for maintenance. With the help of actively controlled electromagnets for suspension and guidance, Maglev trains can run at high speeds along track beams without direct contact between the wheels and the tracks, and this can eliminate many disadvantages with the traditional wheel-rail vehicles, such as traction and braking constraints.

Simulation analysis on Maglev systems is a method used to investigate the uneven conditions (track irregularities) of Maglev system, on the one hand, it makes the optimization of dynamic responses under various operating conditions possible, thereby improving operational safety and passenger comfort, on the other hand, it enables researchers to simulate the operation situations of the train under various condition, through which the dynamic responses in various scenarios can be studied, the structural design of the train body and the Maglev system can be optimized,

and the stability and reliability of the trains during operation can be enhanced. For Maglev trains as a high-speed transportation means, the safety issue is of utterly importance, such simulation analysis can discover and study the dynamic responses in various fault scenarios, such as tilting and lateral deviation of the train body, and only in this way, can we make safety assessment and identify potential operational hazards in advance. Moreover, the travelling speed of Maglev trains is much faster than traditional rail transport, and this has placing greater demands on passenger comfort. Simulation analysis can simulate vibrations and noise during high-speed travel, so that optimizations can be made to the shock absorption system and the impact of vibrations and noise on passengers can be reduced, ultimately improving the their ride comfort [2, 3]. In a word, the Maglev track irregularity simulation analysis is of great value in optimizing train design, improving operational safety and comfort, and saving costs and time, so the development and application of this method is of significant importance in the field of Maglev transportation.

In recent years, domestic and international scholars have conducted many studies on the dynamic modeling and simulation of high-speed Maglev trains, and have gained useful results.

Yang et al. [4] proposed a dynamic monitoring and evaluation algorithm for medium and low-speed Maglev tracks. They conducted simulation analyses for various conditions such as track irregularities, single-point height variations, continuous track height changes, rail joint mismatches, and rail joint angles, establishing a high linear correlation between track irregularities and the calculated surface roughness. Zou et al. [5] analyzed the components of track irregularity stimulation and established a vertical dynamic model of high-speed Maglev vehicles in SIMPACK. They studied the impact of speed, track irregularity wavelength and amplitude, vehicle weight, and primary and secondary suspension parameters on stability, and analyzed sensitive wavelength range and the rising trend of vertical Sperling stability on straight tracks at different speeds. Zhang et al. [6] used a virtual stimulation method to develop a rapid calculation algorithm for train stability. They built a single-vehicle dynamic model based on the TR08 Maglev vehicle and used the rapid stability algorithm to analyze the relationship between track irregularity wavelengths and Maglev vehicle stability. They found that lower vertical and lateral stiffness improved stability; higher operational speeds increased the range of track irregularity wavelengths affecting vehicle stability, primarily between 50-100 meters. Phaenkongngam et al. [7] reviewed and designed the propulsion suspension system for Maglev trains. Since Maglev trains are designed with high technology, they may become a normal means of transportation in the future. And because in Thailand, there are very few research projects on magnetic levitation. What is proposed is the construction of a Maglev prototype, which can be preliminarily studied on the Maglev project. Wang et al. [8] used the Universal Mechanism (UM) software to construct a model of high-temperature superconducting (HTS) Maglev axle coupling system, and analyzed its vertical dynamics. Based on the UM model, the vertical dynamics of different bridge spans under different operating speeds were simulated and analyzed. Xia et al. [9] proposed a fast and accurate analysis method for Maglev axle system based on the advantages of theoretical derivation and numerical calculation, and analyzed the influence of bridge and controller on the dynamics of Maglev system. This work aims at the Changsha Maglev Express, in which the mathematical equations for the axle system are proposed. The effect of this parameter on the system was then analyzed. Finally, a vibration test system was built to test the vibration test of the Maglev vehicle bridge through the test scheme, and the experimental results were given. The vibration acceleration test results are in good agreement with the calculation results of the proposed method, which verifies the accuracy of the model and the analysis method. Bruce and Bird [10] analyzes the work by using 2D and 3D dynamic finite element analysis (FEA) modeling, i.e., when the magnetic source moves on an infinitely wide and infinitely long conductive plate guide, the steady-state lateral and translational stiffness terms will be zero, and only the vertically coupled stiffness term needs to be modeled. Using these observations, a simplified 2-degree-of-freedom linearized eddy current dynamic force model can be used to calculate the steady-state force variation of an eddy-current-based Maglev vehicle operating on a wide uniformly conductive track. Floegel-Delor et al. [11] evaluated the current state of bulk superconducting Maglev train technology. The key performance factors such as load, speed, efficiency and environmental protection of existing industrial magnetic trains are pointed out. On this basis, a feasibility analysis should be carried out for the demonstrators trapped in the field train. Abdioglu et al. [12] designed and constructed a new multi-surface (MS) high-temperature superconductor (HTS) magnetic levitation measurement system to investigate the enhanced magnetic properties of magnetic levitation systems over conventional permanent magnet rails (PMG) by MS HTS configurations. The static and stiffness behavior and dynamic response characteristics of these MS HTS-PMG configurations at different on-site cooling heights (FCH) were investigated. Shi et al. [13] redesigned the suspension bogies of TR series Maglev trains, adding an intermediate buffer layer and suspension modules between the bogies to improve curve passing capability and reduce vertical dynamic coupling effects between the vehicle and the track beam. They constructed a new type of dynamic model for Maglev vehicles, conducted computer simulation analyses comparing old and new bogie track dynamic models, and found that the redesigned suspension bogie structure had minimal dynamic interaction with the track beam, indicating an improved operational environment for the electromagnets in the new Maglev trains.

In summary, the prevailing research predominantly concentrates on Maglev train-bridge coupled systems operating at speeds up to 400 km/h. These studies utilize numerical and modeling simulation methods to investigate system

vibrations at resonance speeds. Key focus areas include analyzing system parameters such as primary and secondary vertical stiffness and damping, suspension gap, and track irregularity wavelengths, leading to the proposal of various optimization strategies. However, these studies primarily operate at relatively lower speed levels, mainly considering the effects of track irregularities and speed on the vehicle's overall dynamic characteristics. There is a notable gap in research regarding the stability changes and sensitivity of high-speed Maglev trains operating at speeds exceeding 500 km/h. This deficiency poses a significant obstacle to the advancement of high-speed Maglev technology in China. Consequently, there is an imperative need to develop and utilize simulation models to investigate the responses of Maglev trains and variations in their smoothness indices under diverse operating conditions.

2 Dynamics Modeling and Parameters of High-Speed Maglev Train

2.1 Single Electromagnet Suspension Control Model

According to the electromagnetic suspension modes, Maglev trains can be categorized into four types of suspension methods: Electromagnetic Suspension (EMS), Electrodynamic Suspension (EDS), Permanent Magnet Suspension (PMS), and High-Temperature Superconducting Magnetic Suspension (HTS). Additionally, there are hybrid electromagnetic suspension methods combining these four types.

The TR08 type Maglev train employs the EMS system, where dedicated electromagnets are responsible for suspension and guidance, divided into suspension electromagnets and guidance electromagnets. Each suspension frame is equipped with multiple independently controllable suspension and guidance electromagnets.

The control of suspension and guidance electromagnets constitutes the basic unit of Maglev train control. Each control unit can be described by a single electromagnet suspension control model. The single electromagnet suspension control model is illustrated in Figure 1.

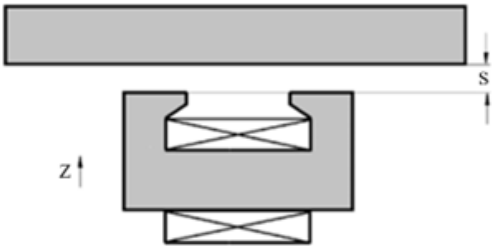

Figure 1. Single electromagnet suspension control model

In Maglev simulation analysis, the single electromagnet suspension control model is most commonly used. Under the assumption of neglecting the magnetic resistance of the magnetic conductor and leakage flux in the electromagnetic circuit, the formula for calculating electromagnetic force is as follows:

$$F = \kappa \left(\frac{I}{S} \right)^2 \tag{1}$$

where, I represents the current, S represents the air gap (suspension gap or guidance gap), and κ represents the electromagnet constant.

The value of κ can be calculated using the following formula:

$$\kappa = \frac{\mu_0 A N^2}{4} \tag{2}$$

where, μ_0 represents the vacuum permeability, A represents the effective magnetic pole area, and N represents the number of turns in the electromagnet coil. Since these three quantities are constants, κ is also a constant.

According to Kirchhoff's voltage law, the circuit voltage equation for the single-stage electromagnet model is:

$$\frac{d(LI)}{dt} = -RI + U \tag{3}$$

Namely

$$L\dot{I} + \dot{L}I = -RI + U \tag{4}$$

where, R is the coil resistance, I is the electromagnet current, and U is the electromagnet voltage. The inductance L has the following relationship with the air gap S and the electromagnetic force constant κ:

$$L = \frac{\kappa}{2S} \tag{5}$$

By Substituting Eq. (5) into the voltage Eq. (4) of the single electromagnet model, we get:

$$L\dot{I} = -RI + \frac{LI}{S}\dot{S} + U \tag{6}$$

In considering the steady state of the single electromagnet suspension control model, it's customary to let F_0 be the rated electromagnetic force and S_0 the rated air gap. Hence, using these two known quantities as constants to calculate other variables, we can get the rated current I_0, rated voltage U_0, and rated inductance L_0:

$$I_0 = S_0\sqrt{\frac{F_0}{\kappa}} \tag{7}$$

$$U_0 = RI_0 \tag{8}$$

$$L_0 = \frac{\kappa}{2S_0} \tag{9}$$

The single electromagnet suspension control model provided in UM employs a PID (Proportional-Integral-Derivative) voltage control model with displacement, velocity, and acceleration feedback. Its voltage control equation is:

$$\begin{gathered} U = U^0 + U_s\Delta S + U_v\dot{S} - U_a\ddot{Z} + U_{is}\int_0^t \Delta S dt \\ \Delta S = S - S_0 \end{gathered} \tag{10}$$

The increase in the vertical coordinate of the electromagnet is opposite to the direction of the air gap, as shown in Figure 1.

If the integral part is not considered, namely $U_{is} = 0$, then the initial voltage U^0 is equal to the rated voltage $U_0, U^0 = U_0 = RI_0$.

By simplifying the voltage control equation and substituting Eq. (6) into Eq. (10), we get:

$$L\dot{I} = -RI + U^0 + U_s\Delta S + \left(U_v + \frac{LI}{S}\right)\dot{S} + U_{is}\int_0^t \Delta S dt - -U_a\ddot{Z} \tag{11}$$

Thus, the parameters describing the single electromagnet suspension control model are: F_0, S_0, κ, R, U^0, U_s, U_v, U_a, U_{is}. Generally, the first four parameters F_0, S_0, κ, R are constants related to the stable working point. The last four parameters U_s, U_v, U_a, U_{is} are control parameters that need to be set individually.

This model is applicable for the suspension and guidance control of conventional conductive highspeed Maglev trains.

2.2 Full Vehicle Model

As shown in Figure 2, the high-speed Maglev vehicle model established in UM consists of a vehicle body and six suspension frame subsystems. Each suspension frame subsystem contains a frame, two suspension electromagnets, and two guidance electromagnets. There are four acceleration sensors mounted on each electromagnet. A primary suspension system is placed between the electromagnet and the frame, and a secondary suspension system is situated between the vehicle body and the frame. The model encompasses a total of 114 degrees of freedom. The dynamic parameters of the model are presented in Table 1.

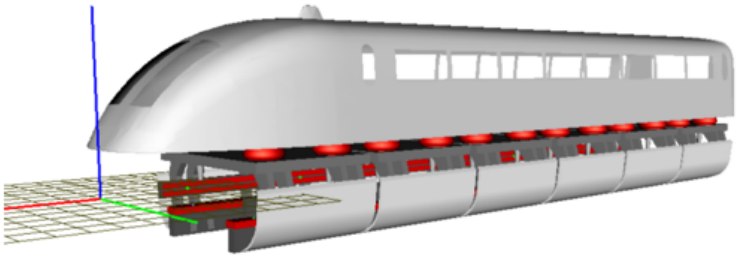

Figure 2. High-speed Maglev train dynamics model

Table 1. Dynamic parameters of the high-speed Maglev train dynamics model

Parameter	Value
Vehicle Body Mass (kg)	15,000
Suspension Frame Mass (kg)	1,000
Suspension/Guidance Electromagnet Mass (kg·m^2)	600
Vehicle Body Moment of Inertia Matrix	diag (5e4, 3e5, 3e5)
Suspension Frame Moment of Inertia Matrix	diag (1000, 1000, 1000)
Suspension/Guidance Electromagnet Moment of Inertia Matrix	diag (20, 600, 600)
Number of Suspension Frames	6
Vertical Stiffness of Air Springs (N/m)	2.00E+05
Lateral/Longitudinal Stiffness of Air Springs (N/m)	1.00E+04
Vertical Damping of Air Springs (N·s/m)	3000
Lateral/Longitudinal Damping of Air Springs (N·s/m)	2000
Spring Preload Force (N)	6131.25
Initial Guidance Force (N) (denoted as fy0)	5000
Initial Suspension Force (kN) (denoted as fz0)	14.46975

2.3 Suspension Frame Model

As depicted in Figure 3, each suspension frame is equipped with 4 air springs, 2 suspension electromagnets, and 2 guidance electromagnets. The connections between the suspension frame and its components are as follows: The suspension electromagnets have degrees of freedom for translational movement along the X and Z axes and rotational movement around the Y axis relative to the frame. At the connection points, stiffness matrices are set with CX = 5e6, CZ = 5e6, CAY = 1e5, DX = 5e4, DZ = 5e4, DAY = 1e3. The guidance electromagnets have degrees of freedom for translational movement along the X and Y axes and rotational movement around the Z axis relative to the frame. At these connection points, stiffness matrices are set with CX = 5e6, CY = 5e6, CAZ = 1e5, DX = 5e4, DY = 5e4, DAZ = 1e3. The top points of the air springs are connected to the vehicle body, while the bottom points are connected to the frame. The total initial preload force of all springs is equal to the gravitational force of the vehicle body.

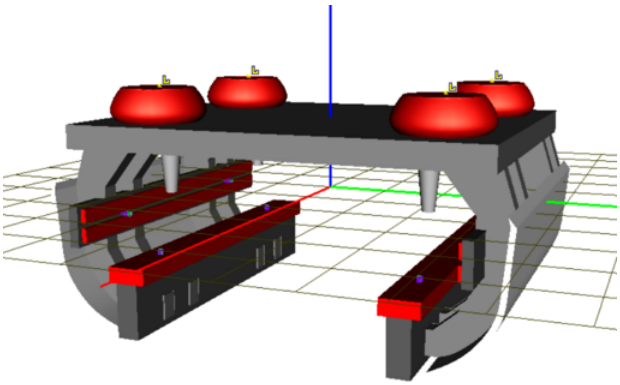

Figure 3. Suspension frame model

Considering the single electromagnet control model for ease of simulation, concentrated forces are uniformly applied at the front and back of each suspension and guidance electromagnet in the Maglev bogie model to represent

electromagnetic forces (as shown by the blue points on the red faces of the suspension and guidance electromagnets in Figure 3). Additionally, gap sensors are installed at the locations where the forces are applied to detect the distance between the electromagnets and the corresponding rail surface, thereby adjusting the magnitude of the electromagnetic force to control the suspension force and guidance force. The initial value of the suspension electromagnetic force is fz0, and the initial value of the guidance force is fy0.

3 Track Irregularity and Stability Index

3.1 Track Irregularit

Track irregularity power spectrum plays a significant role in vehicle dynamics. Random irregularities are a universal source of excitation, which can be derived from existing airport runway and highway Power Spectral Density (PSD) functions, railway PSD functions, or directly measured track irregularity data [14–18].

Track irregularity is categorized into periodic track irregularity, track slope irregularity, and track step irregularity. These types of irregularities can adversely affect the suspension control system of Maglev trains. Numerous domestic and international experts and scholars have conducted research on the impact of track irregularity on Maglev train suspension control systems. For periodic track irregularity, the bent track beam is assumed to represent periodic track irregularity and is expressed using a sine function [19–21].

To select different types of irregularity excitation under rigid track beam conditions for the guidance surface, the construction of the guidance surface irregularity primarily involves three typical functions - sine, ramp, and step – as the irregularity excitation. To facilitate the investigation of the impact of different irregularities on the suspension surface of Maglev trains, no irregularity excitation will be applied to the left and right suspension surfaces. For the left and right guidance surfaces, due to their opposite orientations, opposite irregularity excitations should be applied to reflect the changes in the line. Below is an explanation of the rationale for constructing the irregularity conditions and the display of the irregularity waveforms.

3.1.1 Sine excitation

In consideration of track beam deformation due to thermal expansion, resulting in an upward arching in the horizontal direction, the left guidance surface becomes convex and the right guidance surface becomes concave. The deformation is shaped like a half sine wave with a span length of 24m and an amplitude of 1mm. The waveform of the irregularity is shown in Figure 4, where the blue line represents the irregularity excitation of the left guidance surface, and the red line represents the irregularity excitation of the right guidance surface.

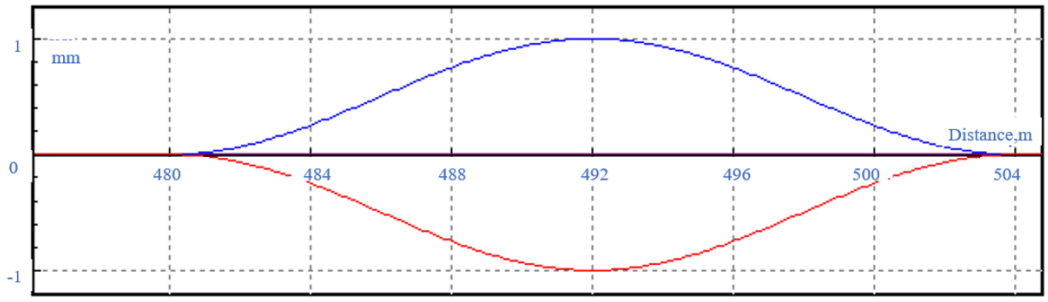

Figure 4. Spectrum of sine excitation irregularity

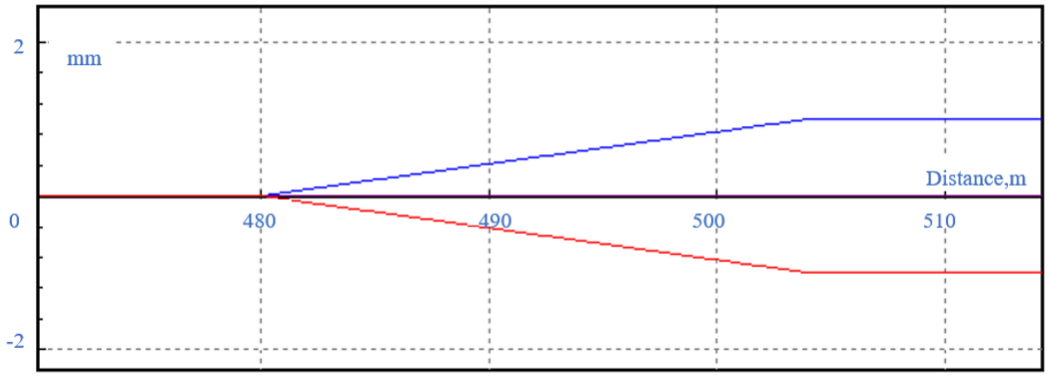

Figure 5. Spectrum of ramp excitation irregularity

3.1.2 Ramp excitation

Taking into account construction errors in track beams, which cause irregularities in the track direction, the guidance surfaces are subjected to a ramp excitation with a deviation of 1mm over a span length of 24m. The waveform of the irregularity is depicted in Figure 5, where the blue line indicates the irregularity excitation of the left guidance surface, and the red line represents the irregularity excitation of the right guidance surface.

3.1.3 Step excitation

Considering construction errors in track beams, a step excitation occurs at the joint between two track beams, affecting the guidance surfaces with a deviation of 0.4mm. The waveform of the irregularity is displayed in Figure 6, where the blue line denotes the irregularity excitation of the left guidance surface, and the red line indicates the irregularity excitation of the right guidance surface.

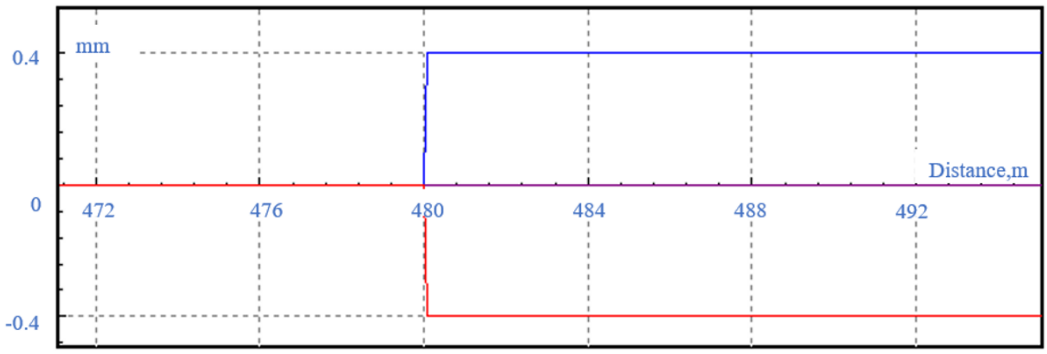

Figure 6. Spectrum of step excitation irregularity

3.2 Stability Index

Stability index is a method used to measure the comfort of passengers and crew aboard locomotive vehicles, as well as the integrity of transported goods [22]. The operational stability of trains is evaluated using the Sperling Comfort Index. The stability index for rail vehicles is divided into three levels: Level 1, Level 2, and Level 3. Level 1 corresponds to a stability index of $\leq$2.50, indicating an excellent stability rating for the rail vehicle. Level 2 corresponds to a stability index of $>$2.50 and $\leq$2.75, indicating a good stability rating. Level 3 corresponds to a stability index of $>$2.75 and $\leq$3.00, indicating an acceptable stability rating.

4 Simulation Results

The control parameters for the electromagnetic force on the guidance surface are chosen as follows: initial electromagnetic force fy 0=5(kN), initial voltage $U_0 = 7.07(\ \mathrm{V})$, resistance $\mathrm{R} = 1(\Omega)$, and electromagnetic force control parameters $U_s = 2000(\ \mathrm{V/m}), U_{is} = 1500(\ \mathrm{V/ms}), U_v = 1000(\mathrm{Vs/m}), U_a = 4\left(\mathrm{Vs^2/m}\right)$. The initial gap S_0 is set at $10\ \mathrm{mm}$ regardless of the speed [23, 24].

Since there is only one irregularity excitation at a specific point on the guidance surface, preliminary experiments revealed that the magnitude of vertical acceleration is only at the 10^{-5} level. Our focus is on the lateral acceleration response of the Maglev train under this excitation, the lateral stability index, the time taken to return to a steady state (convergence time), and the changes in the guidance gap under this excitation.

4.1 Sine Excitation

The time-domain diagram of lateral acceleration is used to analyze the motion characteristics and driving stability of the vehicle. In a time-domain graph, lateral acceleration represents the change in the acceleration of a vehicle in the lateral direction. It can be seen from Figure 7, the transverse acceleration of the car body reaches its peak acceleration of 0.18m/s2 at 3.3s at the speed of 600km/h under the sinusoidal excitation condition, and the transverse acceleration fluctuates smoothly after 5s.

Maglev train is a train system that uses Maglev technology to achieve levitation and propulsion. Due to the unique magnetic principle of the guidance system of the Maglev train, the analysis of the guide gap fluctuation diagram is very important to evaluate its operational stability and driving performance. In the guide clearance fluctuation diagram of a Maglev train, the horizontal axis represents the time, and the vertical axis represents the amount of change in the guide clearance. It can be seen from Figure 8, the fluctuation amplitude reaches the maximum at 3.05s at the 600 km/h speed under sinusoidal excitation condition, then gradually decreases, and tends to stabilize after 4.8s.

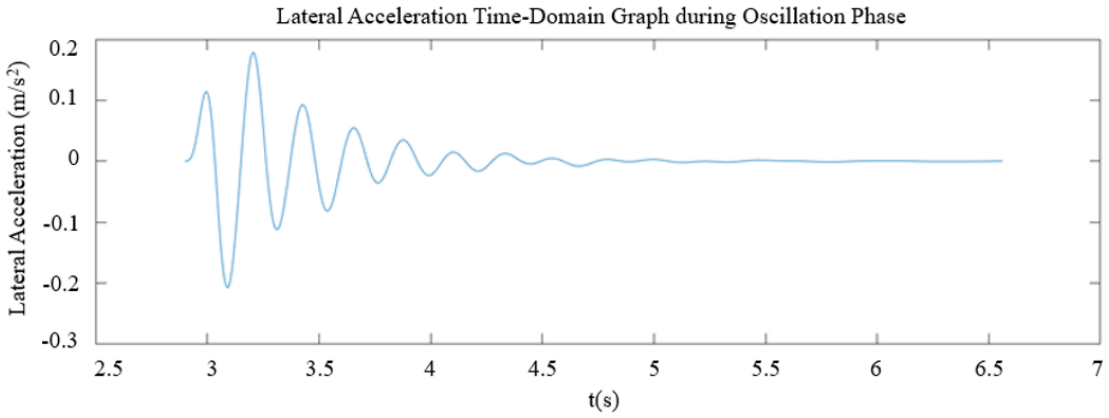

Figure 7. Lateral acceleration response of the vehicle at 600 km/h under sine excitation

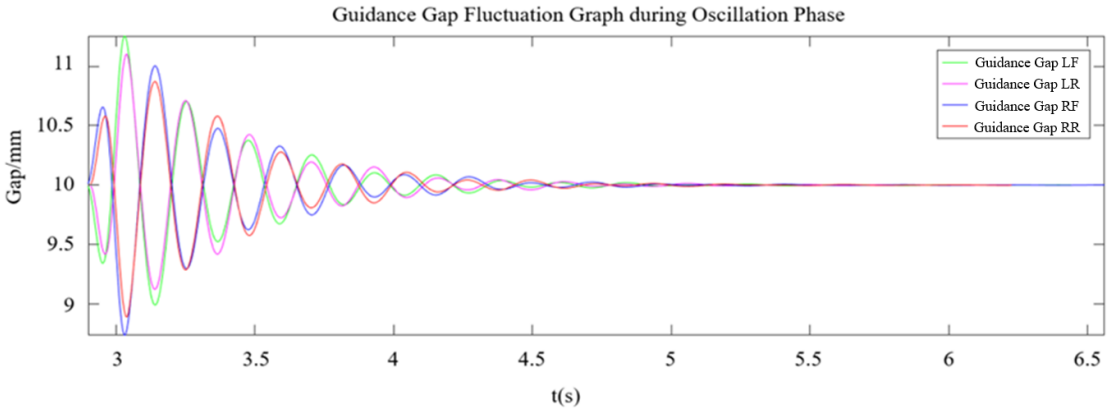

Figure 8. Guidance gap response at 600 km/h under sine excitation conditions

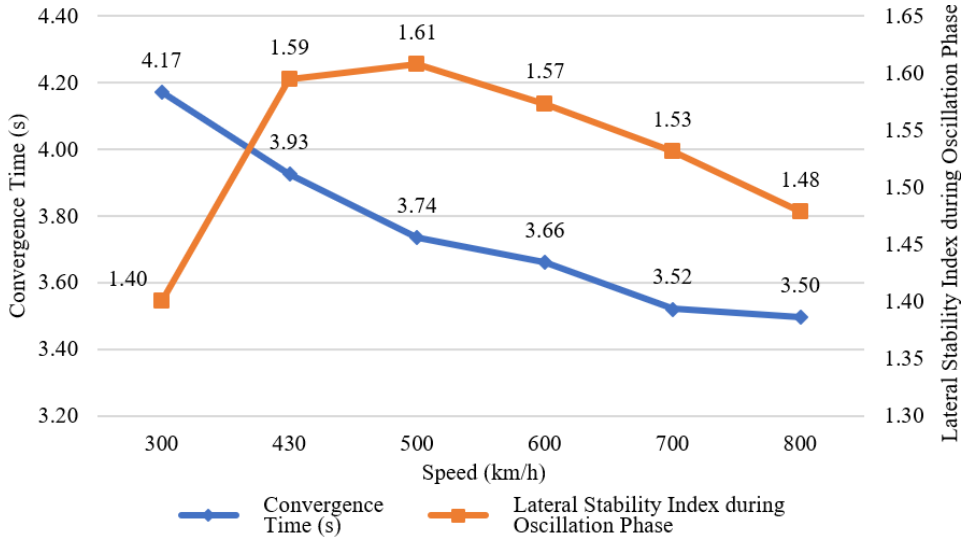

Figure 9. Convergence time and lateral stability index during oscillation phase under sine excitation conditions

From Figure 9, it can be observed that under the sine excitation irregularity waveform, as the speed of the Maglev train increases from 300 km/h to 430 km/h, the lateral stability index rapidly rises from 1.40 to 1.59. As the speed further increases from 430 km/h to 500 km/h, the lateral stability index shows a slow increase, moving from 1.59 to 1.61. When the speed increases from 500 km/h to 800 km/h, the lateral stability index subsequently decreases from 1.61 to 1.48. The convergence time decreases as the linear speed of the train increases.

From Figure 10, it is evident that under the sine excitation irregularity waveform, as the operational speed increases from 300 km/h to 430 km/h, there is a notable increase in the maximum value of the train's guidance gap,

rising from 10.9mm to 11.2mm. As the speed further increases from 430 km/h to 800 km/h, there is some fluctuation in the maximum value of the guidance gap, with a slight decrease, but it is not significant. The minimum value of the train's guidance gap decreases significantly as the speed increases from 300 km/h to 430 km/h, dropping from 9.09mm to 8.79mm. As the speed increases from 430 km/h to 800 km/h, the minimum value of the guidance gap experiences fluctuations and a slight increase, but this change is not significant.

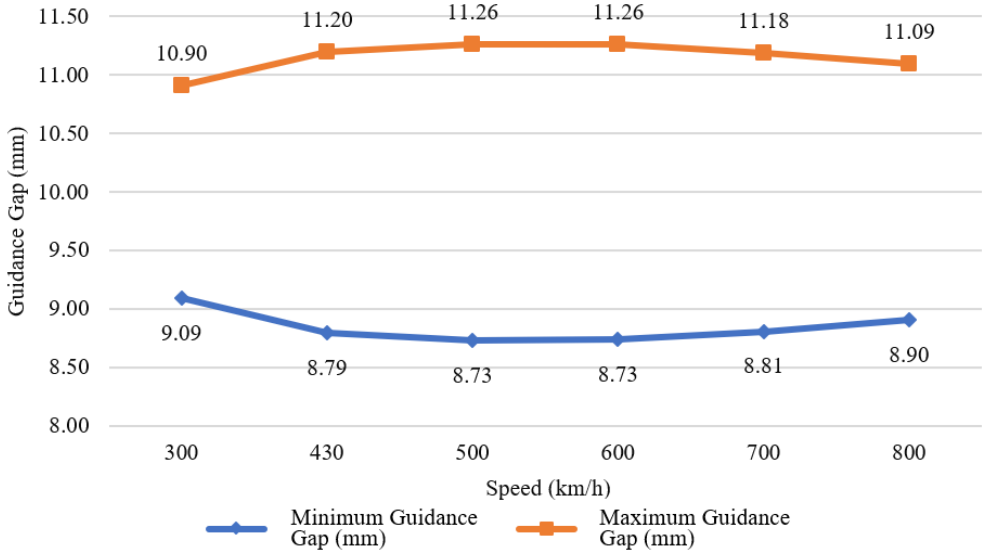

Figure 10. Guidance gap under sine excitation conditions

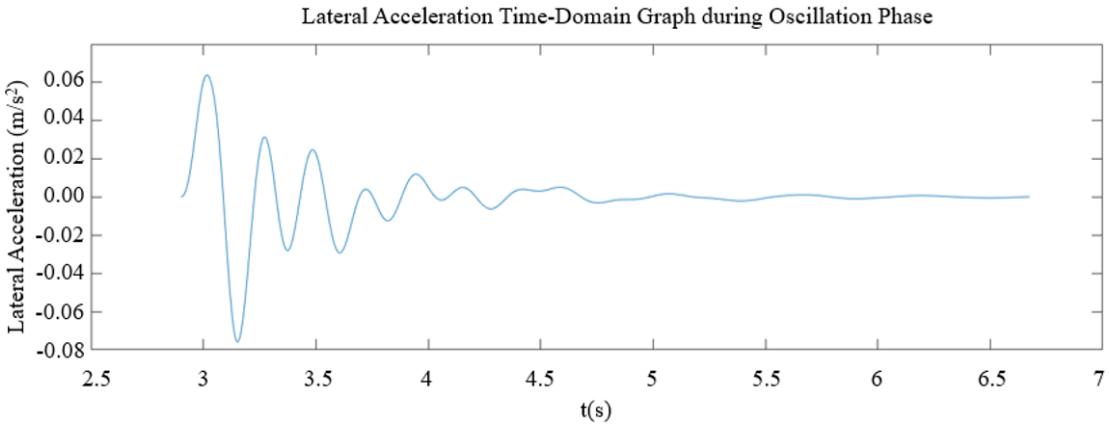

Figure 11. Lateral acceleration response of the vehicle at 600 km/h under ramp excitation conditions

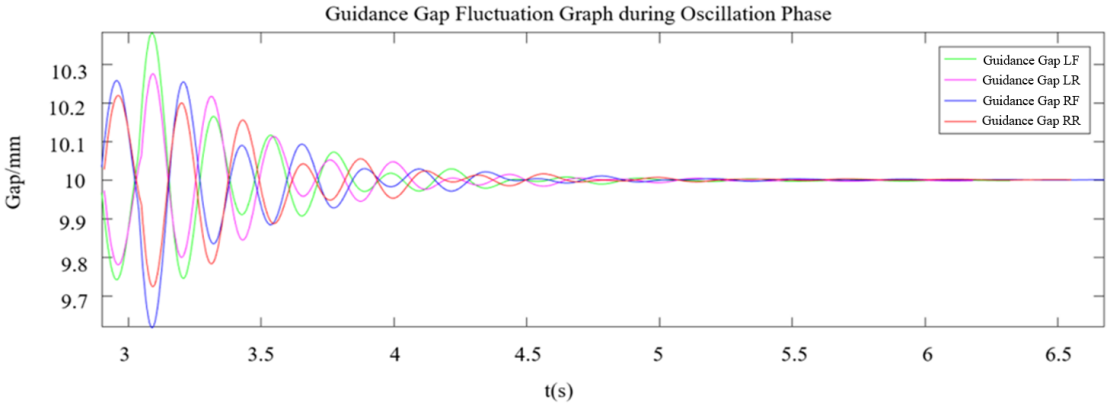

Figure 12. Guidance gap response at 600 km/h under ramp excitation conditions

4.2 Ramp Excitation

It can be seen from Figure 11, the lateral acceleration of the vehicle body reaches its peak acceleration of $0.62m/s^2$ at 3.1s at the speed of 600km/h under the slope excitation condition, and the transverse acceleration fluctuates smoothly after 5s. And From Figure 12, the fluctuation amplitude reaches the maximum at 3.05s at the 600 km/h speed under the slope excitation condition, then decreases gradually, and tends to stabilize after 4.9s.

From Figure 13, it can be observed that under the ramp excitation irregularity waveform, as the speed of the Maglev train increases from 300 km/h to 800 km/h, the lateral stability index steadily increases from 0.86 to 1.20. As the train's speed increases from 300 km/h to 500 km/h, the convergence time rapidly increases from 3.53s to 3.81s. The peak convergence time of 3.81s is reached at a speed of 500 km/h, after which it decreases with increasing speed, finally settling at 3.74s at 800 km/h.

From Figure 14, under the ramp excitation irregularity waveform, as the operational speed increases from 300 km/h to 800 km/h, the maximum value of the guidance gap increases from 10.14mm to 10.52mm, and the minimum value of the guidance gap decreases from 9.86mm to 9.48mm.

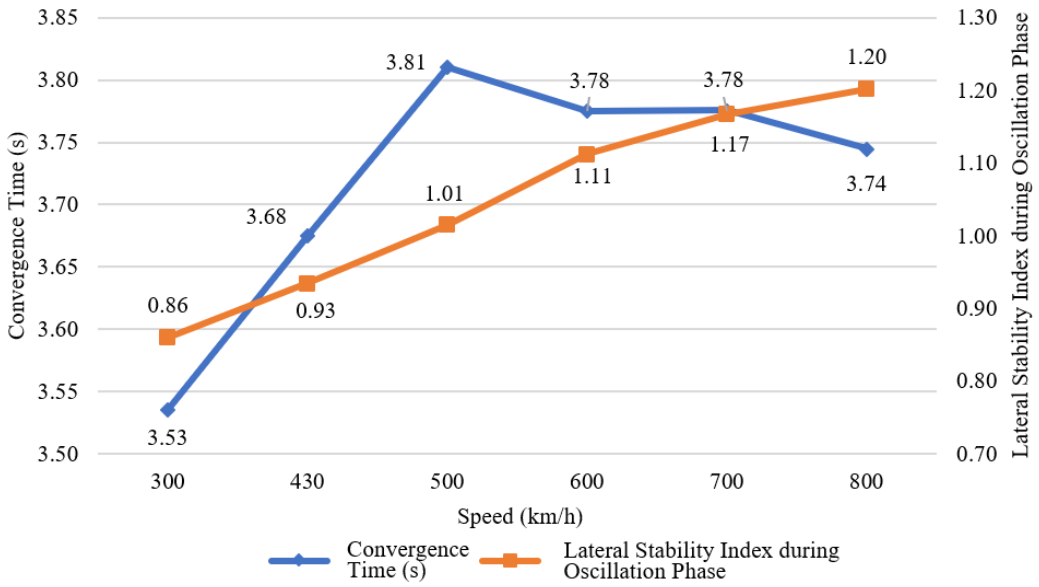

Figure 13. Convergence time and lateral stability index during the oscillation phase under ramp excitation conditions

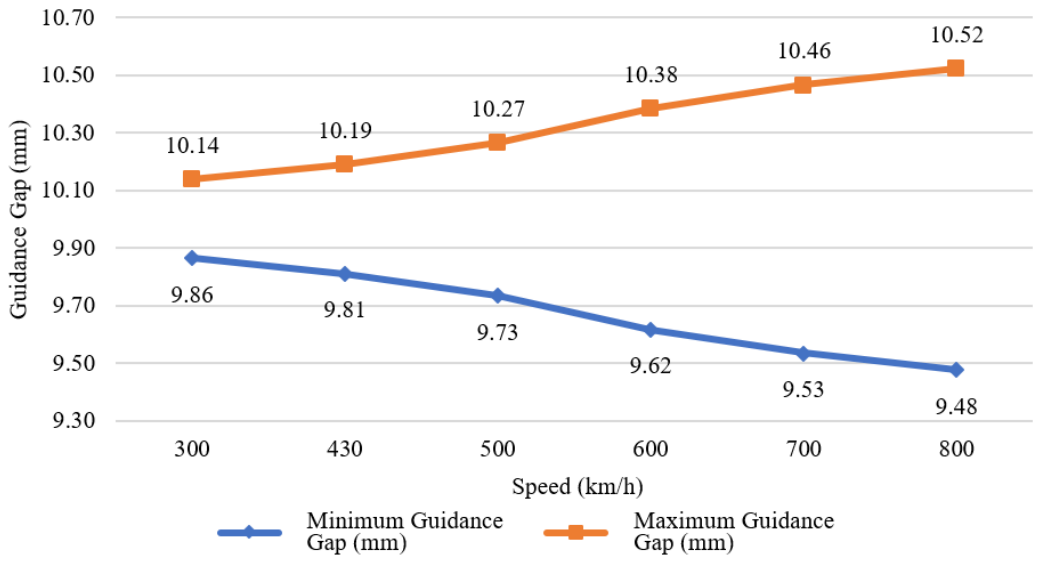

Figure 14. Guidance gap under ramp excitation conditions

4.3 Step Excitation

It can be seen from Figure 15 that the lateral acceleration of the car body reaches its peak acceleration of $0.18m/s^2$ in 3s at the speed of 600km/h under the step excitation condition, and the transverse acceleration fluctuates smoothly after 4.6s. And from Figure 16, the fluctuation amplitude reaches the maximum at the beginning at the 600 km/h speed under the step excitation condition, then decreases gradually, and tends to stabilize after 4.6s.

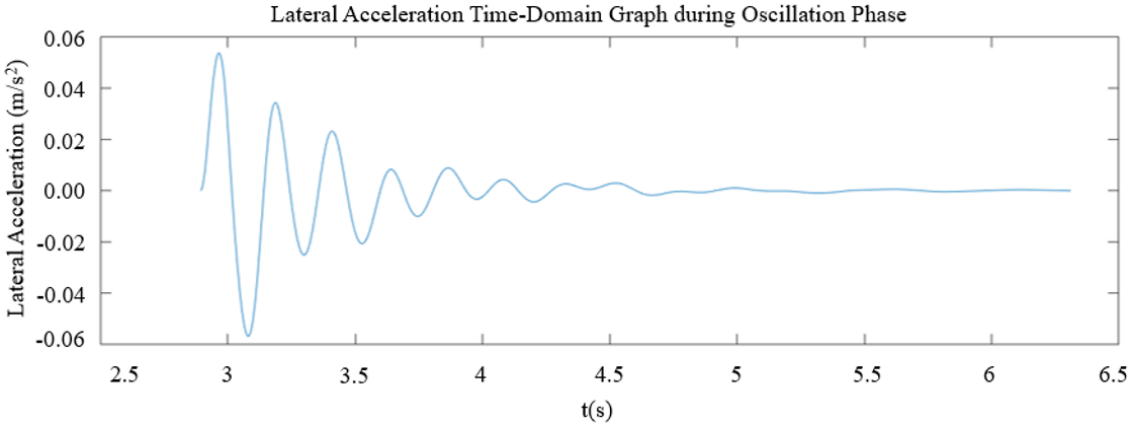

Figure 15. Lateral acceleration response of the vehicle at 600 km/h under step excitation conditions

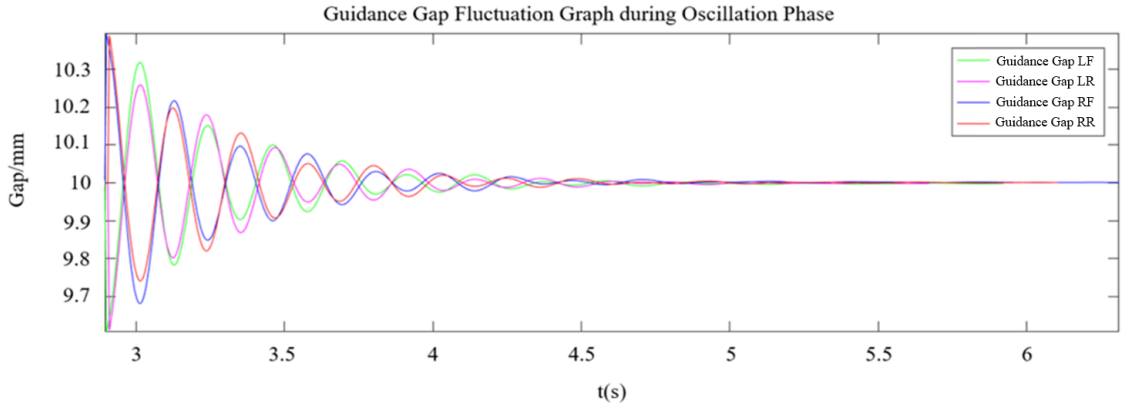

Figure 16. Guidance gap response at 600 km/h under step excitation conditions

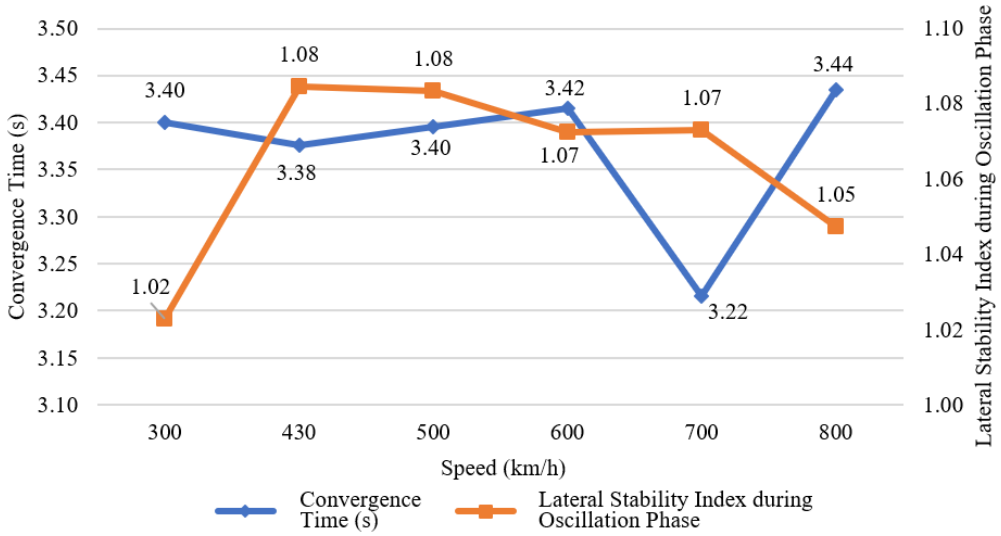

Figure 17. Convergence time and lateral stability index during the oscillation phase under step excitation conditions

From Figure 17, it is evident that under the step excitation irregularity waveform, as the speed of the Maglev train increases from 300 km/h to 430 km/h, the lateral stability index increases from 1.02 to 1.08. As the speed further increases from 430 km/h to 800 km/h, the lateral stability index decreases from 1.08 to 1.05. The convergence time fluctuates around 3.40s as the speed increases from 300 km/h to 600 km/h. When the train speed increases from 600 km/h to 700 km/h, the convergence time decreases from 3.42s to 3.22s. Subsequently, as the train speed increases to 800 km/h, the convergence time rises to 3.44s.

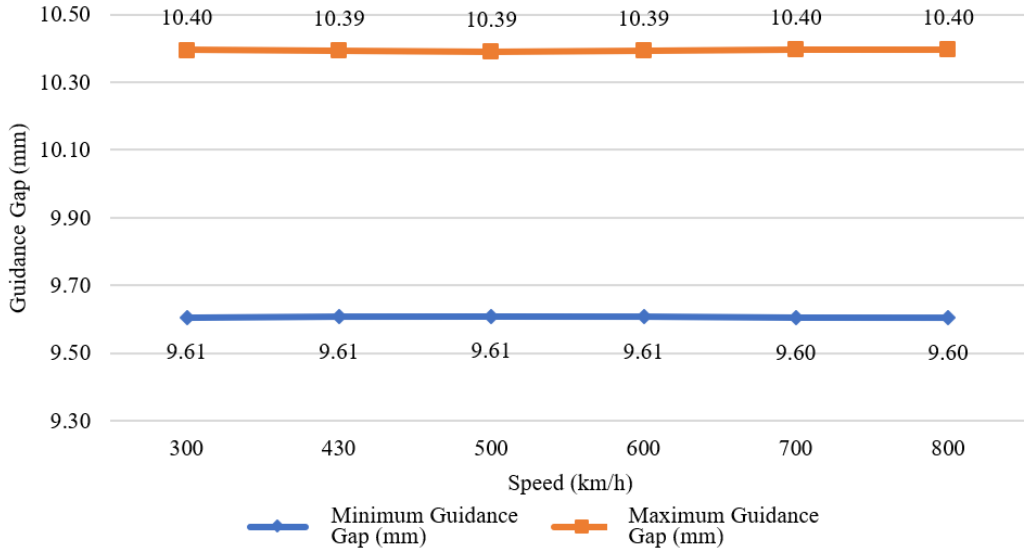

Figure 18. Guidance gap under step excitation conditions

From Figure 18, under the step excitation irregularity waveform, as the operational speed increases, the maximum value of the guidance gap fluctuates between 10.39mm and 10.40mm, showing no significant change. Similarly, as the speed increases, the minimum value of the guidance gap fluctuates between 9.60mm and 9.61mm, also displaying no significant change.

5 Conclusion

High-speed Maglev trains are a new type of rail transport with promising development prospects and are extremely suitable for constructing transportation networks in large urban agglomerations. However, there has been limited research on the dynamic response and stability of high-speed Maglev trains at high speeds. This paper, using the TR08 type high-speed Maglev train on the Shanghai Maglev Demonstration Line as a prototype and employing UM, has established a dynamic model of high-speed Maglev trains. Simulation studies on different types of irregularity structures were conducted, with the main research contents and conclusions as follows:

(1) The structure of the TR08 type high-speed Maglev train was analyzed, and a realistic dynamic model of high-speed Maglev trains was established in UM. The single electromagnet control model was used to control changes in guidance force.

(2) Sine function, ramp function, and step function irregularity waveforms were constructed. Using the established high-speed Maglev train dynamic model, the dynamic response of the Maglev train under rigid track beam conditions at different speeds to these irregularity excitations was simulated. Various changes, including the Sperling stability index, were analyzed. The analysis of the simulation results led to the following conclusions: The lateral stability index of the vehicle body is only affected by the direction of irregularity on the guidance surface. The simpler (or more complex) the shape, and the shorter (or longer) the span and smaller (or larger) the amplitude of a single irregularity excitation, the smaller (or larger) the train's stability index. The fluctuation of the guidance gap, with increasing speed, does not significantly increase. The shorter the span of the guidance surface excitation, the less impact the change in operating speed has on the guidance gap. The situation where the lateral stability index under sine excitation first increases and then decreases with speed, after analysis, is found to be related to the frequency composition of the vehicle body's lateral acceleration. The stability index of the Maglev train, under a single irregularity excitation, may first decrease and then increase with speed. This could be due to the rightward shift of the main component of the acceleration frequency as the speed increases, leading to a decrease in the frequency correction factor; or it could also be the influence of coupled vibrations. At different speeds, the response of high-speed Maglev trains to track irregularities shows significant differences. As the speed increases, the sensitivity of Maglev trains to track irregularities significantly increases, and the Sperling stability index also shows corresponding

changes. These research results provide useful references for the design optimization of high-speed Maglev vehicles and the control of track irregularities, further enhancing the safety and comfort of Maglev train operation.

Data Availability

The data used to support the findings of this study are available from the corresponding author upon request.

Conflicts of Interest

The authors declare that they have no conflicts of interest.

References

[1] G. Shu, R. Meisinger, and G. Shen, "Simulation of a MAGLVE train with periodic guideway deflections," in *2008 Asia Simulation Conference - 7th International Conference on System Simulation and Scientific Computing*, Beijing, China, 2008, pp. 421–425. https://doi.org/10.1109/ASC-ICSC.2008.4675397

[2] R. R. Song, W. H. Ma, and Z. L. Chen, "An improved expert intelligent PID control in maglve transportation system with different track irregularities," *Appl. Mech. Mater.*, vol. 409, pp. 1141–1146, 2013. https://doi.org/10.4028/www.scientific.net/AMM.409-410.1141

[3] Y. Wang, Y. Qin, and X. Wei, "Track irregularities estimation based on acceleration measurements," in *Proceedings of 2012 International Conference on Measurement, Information and Control*, Harbin, China, 2012, pp. 83–87. https://doi.org/10.1109/MIC.2012.6273305

[4] M. Yang, G. Lin, and S. Bi, "Detection algorithm and simulation of the track irregularity for medium and low-speed Maglve train," *Urban Mass Transit*, vol. 21, no. 12, pp. 101–105, 2018. https://doi.org/10.16037/j.1007-869x.2018.12.023

[5] Y. Zou, F. Liu, Z. Pang, Y. Tang, and T. Wu, "Vertical dynamics simulation of high speed Maglve vehicle under track irregularity excitation," *Mech. Sci. Technol. Aerosp. Eng.*, vol. 40, no. 2, pp. 281–286, 2021. https://doi.org/10.13433/j.cnki.1003-8728.20200041

[6] X. Zhang, J. Zhou, D. Li, and L. Pan, "An optimum analysis of the ride quality of Maglve vehicle," *Urban Mass Transit*, vol. 12, no. 1, pp. 34–39, 2009. https://doi.org/10.3969/j.issn.1007-869X.2009.01.009

[7] T. Phaenkongngam, K. Chinnawong, N. Patumasuit, and C. Techawatcharapaikul, "Reviewing propulsion & levitation system for magnetic levitation train," in *2021 9th International Electrical Engineering Congress (iEECON)*, Pattaya, Thailand, 2021, pp. 185–188. https://doi.org/10.1109/iEECON51072.2021.9440283

[8] H. Wang, Z. Deng, S. Ma, R. Sun, H. Li, and J. Li, "Dynamic simulation of the HTS maglve vehicle-bridge coupled system based on levitation force experiment," *IEEE Trans. Appl. Supercond.*, vol. 29, no. 5, pp. 1–6, 2019. https://doi.org/10.1109/TASC.2019.2895503

[9] W. Xia, J. Zeng, F. Dou, and Z. Long, "Method of combining theoretical calculation with numerical simulation for analyzing effects of parameters on the maglve vehicle-bridge system," *IEEE Trans. Veh. Technol.*, vol. 70, no. 3, pp. 2250–2257, 2021. https://doi.org/10.1109/TVT.2021.3061280

[10] C. Bruce and J. Z. Bird, "An examination of the stiffness terms needed to model the dynamics of an eddy current based maglve vehicle," *IEEE Trans. Magn.*, vol. 59, no. 11, pp. 1–6, 2023. https://doi.org/10.1109/TMAG.2023.3287512

[11] U. Floegel-Delor, P. Schirrmeister, T. Riedel, R. Koenig, V. Kantarbar, M. Liebmann, and F. N. Werfel, "Mobile HTS bulk devices as enabling ton-force technology for Maglev trains," *IEEE Trans. Appl. Supercond.*, vol. 29, no. 5, pp. 1–5, 2019. https://doi.org/10.1109/TASC.2019.2897216

[12] M. Abdioglu, K. Ozturk, M. Ekici, B. Savaskan, S. Celik, and A. Cansiz, "Design and experimental studies on superconducting maglev systems with multisurface HTS–PMG arrangements," *IEEE Trans. Appl. Supercond.*, vol. 31, no. 6, pp. 1–7, 2021. https://doi.org/10.1109/TASC.2021.3085243

[13] Y. Shi, W. Ma, M. Li, and Z. Xu, "Research on dynamics of a new high-speed maglev vehicle," *Veh. Syst. Dyn.*, vol. 60, no. 3, pp. 721–742, 2020. https://doi.org/10.1080/00423114.2020.1838568

[14] H. Xia and N. Zhang, "Dynamic analysis of railway bridge under high-speed trains," *Comput. Struct.*, vol. 83, no. 23-24, pp. 1891–1901, 2005. https://doi.org/10.1016/j.compstruc.2005.02.014

[15] Y. Li, D. Zhou, P. Cui, P. Yu, Q. Chen, L. Wang, and J. Li, "Dynamic performance optimization of electromagnetic levitation system considering sensor position," *IEEE Access*, vol. 8, pp. 29 446–29 455, 2020. https://doi.org/10.1109/ACCESS.2020.2972341

[16] T. Zhang, "Motion simulation of 600 km/h high-speed Maglev train under the condition of multiple groups," in *2022 IEEE 6th Information Technology and Mechatronics Engineering Conference (ITOEC)*, Chongqing, China, 2022, pp. 1208–1214. https://doi.org/10.1109/ITOEC53115.2022.9734403

[17] X. Liu, P. Zhu, Z. Li, S. Liang, and X. Li, "Performance evaluation of maglev train suspension system based on data drive," in *2022 34th Chinese Control and Decision Conference (CCDC)*, Hefei, China, 2022, pp. 1763–1768. https://doi.org/10.1109/CCDC55256.2022.10034332

[18] F. Ni, S. Mu, J. Kang, and J. Xu, "Robust controller design for maglev suspension systems based on improved suspension force model," *IEEE Trans. Transp. Electrific.*, vol. 7, no. 3, pp. 1765–1779, 2021. https://doi.org/10.1109/TTE.2021.3058137

[19] H. K. Liu and X. Zhang, "Maglev control algorithm adapted to variety of track curve," *J. Syst. Simul.*, vol. 22, no. 5, pp. 1101–1105, 2010.

[20] D. Sharma, S. B. Shukla, and S. K. Ghosal, "Modelling and state estimation for control of magnetic levitation system via a state feedback based full order observer approach," *IOP Conf. Ser. Mater. Sci. Eng.*, vol. 377, no. 1, p. 012156, 2018. https://doi.org/10.1088/1757-899X/377/1/012156

[21] G. He, J. Li, and P. Cui, "Nonlinear control scheme for the levitation module of Maglev train," *J. Dyn. Syst. Meas. Control.*, vol. 138, no. 7, p. 074503, 2016. https://doi.org/10.1115/1.4033316

[22] "Specification for evaluation and test evaluation of dynamic performance of rolling stock: GB/T 5599-2019," National Railway Administration of the People's Republic of China, Beijing, Tech. Rep., 2019.

[23] Y. Sun, S. Wang, Y. Lu, J. Xu, and S. Xie, "Control of time delay in magnetic levitation systems," *IEEE Magn. Lett.*, vol. 13, pp. 1–5, 2021. https://doi.org/10.1109/LMAG.2021.3123909

[24] Y. Sun, S. Xie, J. Xu, and G. Lin, "A robust levitation control of maglev vehicles subject to time delay and disturbances: Design and hardware experimentation," *Appl. Sci.*, vol. 10, no. 3, p. 1179, 2020. https://doi.org/10.3390/app10031179